Importance of In-Plane Anisotropy in the Quasi-Two-Dimensional Antiferromagnet $BaNi_2V_2O_8$

W. Knafo,[1,2] C. Meingast,[1] K. Grube,[1] S. Drobnik,[1,2] P. Popovich,[1,2] P. Schweiss,[1] P. Adelmann,[1] Th. Wolf,[1] and H. v. Löhneysen[1,2]

[1]*Forschungszentrum Karlsruhe, Institut für Festkörperphysik, D-76021 Karlsruhe, Germany*
[2]*Physikalisches Institut, Universität Karlsruhe, D-76128 Karlsruhe, Germany*

(Received 14 December 2006; published 27 September 2007)

The phase diagram of the quasi-two-dimensional antiferromagnet $BaNi_2V_2O_8$ is studied by specific heat, thermal expansion, magnetostriction, and magnetization for magnetic fields applied perpendicular to **c**. At $\mu_0 H^* \simeq 1.5$ T, a crossover to a high-field state, where $T_N(H)$ increases linearly, arises from a competition of intrinsic and field-induced in-plane anisotropies. The pressure dependences of T_N and H^* are interpreted using the picture of a pressure-induced in-plane anisotropy. Even at zero field and ambient pressure, in-plane anisotropy cannot be neglected, which implies deviations from pure Berezinskii-Kosterlitz-Thouless behavior.

DOI: 10.1103/PhysRevLett.99.137206 PACS numbers: 75.30.Kz, 75.30.Gw, 75.50.Ee

The study of quasi-two-dimensional (2D) magnetic systems [1] continues to be a focus of theoretical and experimental investigations, motivated in large part by the discovery of high-temperature superconductivity in the quasi-2D cuprates. Further, the search for a magnetic system exhibiting true Berezinskii-Kosterlitz-Thouless (BKT) behavior, initially proposed for 2D XY magnetic systems [2], has been elusive and has only been seen in superfluid and superconducting films [3]. Theoretical studies indicate that BKT behavior can also be expected for 2D Heisenberg systems with a small easy-plane XY anisotropy [4]. Two recent experimental papers suggest that $BaNi_2V_2O_8$ may in fact be a physical realization of such a system [5,6]. $BaNi_2V_2O_8$ has a rhombohedral structure (space group $R\bar{3}$) and its magnetic properties arise from a honeycomb-layered arrangement of spins $S = 1$ at the Ni^{2+} sites. The quasi-2D properties are due to a strong antiferromagnetic Heisenberg superexchange J in the NiO honeycomb layers. Long-range antiferromagnetic ordering, which would be precluded in a purely 2D Heisenberg system, sets in below the Néel temperature $T_N \simeq 50$ K [5] because of small additional energy scales, which we include in the following Hamiltonian:

$$\mathcal{H} = -\sum_{i,j} J\mathbf{S}_i \cdot \mathbf{S}_j - \sum_{i,j'} J'\mathbf{S}_i \cdot \mathbf{S}_{j'} + \sum_i D_{XY}(S_i^z)^2 - \sum_i D_{\mathrm{IP}}(S_i^a)^2 - \sum_i \mu_0 \mathbf{H} \cdot \mathbf{S}_i. \quad (1)$$

The planar XY anisotropy $D_{XY} \simeq 1$ meV is a factor of 10 smaller than J [7] and confines the spins to lie within the honeycomb layers (easy plane). If this were the only additional term in Eq. (1), a true BKT transition could be expected within each 2D layer [4]. However, a real crystal is always three dimensional (3D) and a very small interlayer exchange J' ultimately leads to a crossover from 2D to 3D correlations, and then to a 3D ordering transition [4]. The value of J' is unknown for the present case [7]; however, the extremely small signal at T_N in the specific heat [5] suggests that J'/J is very small (typically, J'/J is in the range 10^{-2}–10^{-6} in quasi-2D systems [1]). The in-plane anisotropy D_{IP} is estimated by 4×10^{-3} meV [7] and acts to align the spins along one of the three equivalent hexagonal easy a axes [5]. The last term in Eq. (1) includes the effect of a magnetic field H, which also acts as an effective anisotropy [1,8].

In this Letter, we study the (T, H) phase diagram of $BaNi_2V_2O_8$ for magnetic fields applied within the honeycomb planes. The combination of specific heat, thermal expansion, magnetostriction, and magnetization allows us to calculate the uniaxial pressure dependences of T_N, J, and of a crossover field H^* related to spin alignment. In particular, we find a strong anisotropy of the pressure dependences of T_N in the easy plane, which is related to the spin direction. This directly underlines the importance of the in-plane anisotropy term D_{IP} in Eq. (1) for establishing 3D long-range order in $BaNi_2V_2O_8$. Our analysis and comparison with literature indicates that the obtained (T, H) phase diagram may be generic to quasi-2D antiferromagnets with a degenerate number of easy axes and with $J \gg D_{XY} \gg D_{\mathrm{IP}}, J'$. It would be useful if the theoretical models for quasi-2D Heisenberg systems, which already consider XY anisotropy and interplane coupling [4], would also incorporate this in-plane anisotropy.

Single crystals of $BaNi_2V_2O_8$ (42.8 mg) and $BaNi_{0.8}Mg_{1.2}V_2O_8$ (4.85 mg) were grown in fluxes composed of $BaCO_3$, NiO, MgO, and V_2O_5, using Al_2O_3 crucibles. Specific heat was measured using a physical properties measurement system from quantum design [9]. Thermal expansion and magnetostriction were measured using a high-resolution capacitive dilatometer with temperature and field sweep rates of 20 mK/s and 0.5 T/min, respectively. The cell is rotatable, allowing both longitudinal and transverse measurements. Magnetization was measured using a MPMS from quantum design. For all measurements, the magnetic field was applied parallel to the easy plane.

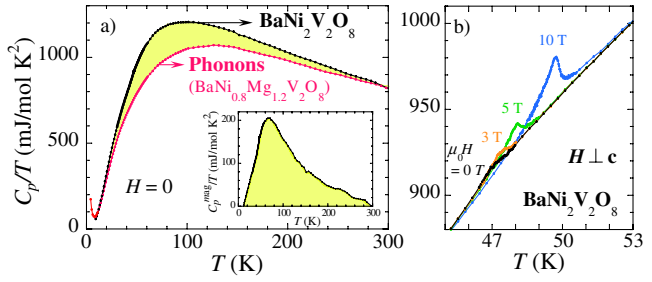

FIG. 1 (color online). (a) Specific heat of $BaNi_2V_2O_8$ and $BaNi_{0.8}Mg_{1.2}V_2O_8$, plotted as C_p/T versus T; the estimated magnetic specific heat of $BaNi_2V_2O_8$ is plotted in the inset. (b) C_p/T versus T of $BaNi_2V_2O_8$ with $H \perp c$.

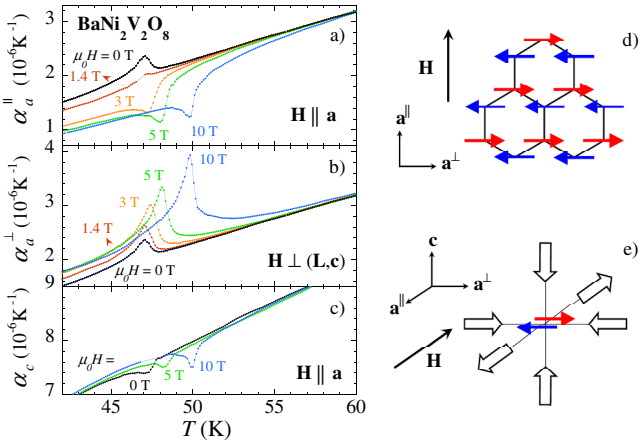

FIG. 2 (color online). (a)–(c) a- and c-axes thermal expansivity of $BaNi_2V_2O_8$ versus temperature, the field being applied parallel to the easy plane, i.e., $H \perp c$. (d),(e) Schematics of the magnetic structure of the Ni^{2+} ions in the plane and of the field-induced lattice distortion (below T_N).

Figure 1(a) shows the 0-T specific heat C_p of $BaNi_2V_2O_8$ in a C_p/T versus T plot. An estimation of the phonon contribution C_p^{ph} is made using the specific heat of $BaNi_{0.8}Mg_{1.2}V_2O_8$ [10]. The resulting magnetic specific heat $C_p^{\mathrm{mag}} = C_p - C_p^{\mathrm{ph}}$ is shown in the inset of Fig. 1(a), where C_p^{mag}/T is plotted as a function of T. The integrated entropy $\Delta S_{\mathrm{mag}} \simeq 24$ J/mol K is roughly equal to the value $2R \ln 3 \simeq 18$ J/mol K expected for the $S = 1$ Ni^{2+} ions. In this plot, there is little signature of the transition at T_N; rather, C_p^{mag}/T has a broad maximum at $T_{\max} \simeq 70$ K which is attributed to the buildup of 2D correlations and corresponds to the highest magnetic energy scale J. Figure 1(b) shows a blowup of the C_p anomaly related to the ordering at T_N. At $H = 0$, we clearly observe a tiny peak yielding $T_N = 47.4 \pm 0.1$ K, defined as the locus of the minimum of $\partial(C/T)/\partial T$ [11]. The magnetic entropy $\Delta S_N \simeq 13$ mJ/mol K gained at T_N is only a tiny fraction of the total magnetic entropy, the very small ratio $\Delta S_N/\Delta S_{\mathrm{mag}} \simeq 7 \times 10^{-4}$ [11] being a consequence of the strong 2D Heisenberg character of the system [12]. Application of a magnetic field in the easy plane leads, at 10 T, to the increases of T_N by about 3 K and of ΔS_N by a factor 4.

The linear thermal expansivity $\alpha = (1/L)\partial L/\partial T$ is shown in Figs. 2(a)–2(c) for T close to T_N and $0 \leq \mu_0 H \leq 10$ T. Data for three configurations are presented: a longitudinal one, $\alpha_a^{\parallel}$ ($\mathbf{L} \parallel \mathbf{H} \parallel \mathbf{a}$), and two transverse ones, $\alpha_a^{\perp}$ [$\mathbf{L} \parallel \mathbf{a}$ and $\mathbf{H} \perp (\mathbf{L}, \mathbf{c})$], and α_c ($\mathbf{L} \parallel \mathbf{c}$ and $\mathbf{H} \parallel \mathbf{a}$). At $H = 0$, T_N is characterized by the jumps $\Delta\alpha_a > 0$ [Figs. 2(a) and 2(b)] and $\Delta\alpha_c < 0$ [Fig. 2(c)]. Application of a magnetic field in the easy plane induces an increase of T_N, defined at the extremum of $\partial\alpha/\partial T$, in agreement with the specific heat data. The field induces a sign change of $\Delta\alpha$ for the longitudinal configuration [Fig. 2(a)], while the sign of $\Delta\alpha$ does not change for the transverse configurations [Figs. 2(b) and 2(c)].

Figure 3 shows the values of T_N extracted from specific heat and thermal expansion. The key observation, which is independent of the direction of H within the hexagonal plane, is that $T_N(H)$ is almost constant for $\mu_0 H \lesssim 2$ T and increases linearly for $\mu_0 H \gtrsim 2$ T. The derivatives of isothermal magnetization and magnetostriction [at $T = 5$ K, see Fig. 4(d)] both show broad peaks, without any measurable hysteresis, at $\mu_0 H^* \simeq 1.5$ T. As seen in Fig. 3, $\mu_0 H^*$ is nearly temperature independent, varying between 1.5 T at 5 K and 2 T near T_N. We interpret H^* as a spin-flop-like crossover field, above which the spins are aligned nearly perpendicular to the field [Fig. 2(e)]. Contrary to a first-order spin-flop transition, which occurs in a single-easy-axis system when H is applied parallel to the spins, a crossover is obtained because of the presence, at zero field, of three kinds of domains, in which the spins are orientated along equivalent hexagonal directions [5]. In addition to the collective rotation of the spins induced by the field, a domain alignment, by domain wall motion, probably plays a crucial role in the alignment of the spins. This crossover may additionally be broadened because of a tiny domain

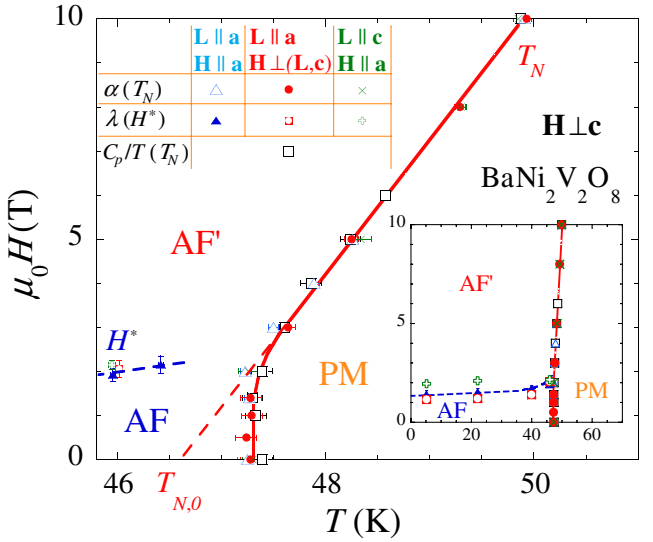

FIG. 3 (color online). Phase diagram obtained with $\mathbf{H} \perp \mathbf{c}$. PM, AF, and AF′ denote the paramagnetic, the low-, and the high-field antiferromagnetic phases, respectively.

wall energy due to the quasi-2D nature of the magnetic exchange [1].

For $\mathbf{H} \perp \mathbf{c}$, the alignment of the spins, which is controlled by the minimization of $|\mathbf{H} \cdot \mathbf{S}|$, can be represented by an effective field-induced Ising in-plane anisotropy $D_{\mathrm{IP}}^{\mathrm{eff}}(\mathbf{H})$ [13], in which the easy axis is perpendicular to ($\mathbf{H}$, $\mathbf{c}$). In the high-field AF' state (Fig. 3), i.e., for $\mu_0 H \gtrsim 2$ T, $D_{\mathrm{IP}}^{\mathrm{eff}}(\mathbf{H})$ dominates over the intrinsic D_{IP} term and the spins are almost perpendicular to $\mathbf{H}$. The linear increase of $T_N(H)$ observed in this regime is related to a reduction of the spin fluctuations along the direction of $\mathbf{H}$, due to the field-induced anisotropy [14]. The high-field line extrapolates to $H = 0$ at $T_{N,0} = 46.6 \pm 0.1$ K, which is smaller than $T_N(H = 0)$ by $\Delta = 0.8 \pm 0.2$ K. Theoretical support is needed to quantitatively relate $T_{N,0}$ and the slope of $T_N(H)$ to the characteristic energy scales of the problem. Nevertheless, we speculate that $T_{N,0}$ is the ordering temperature of the system in the limit of no in-plane anisotropy, i.e., with $D_{\mathrm{IP}} \to 0$ and $H^* \to 0$, so that $T_{N,0}$ is only controlled by J, J', and D_{XY}. In this picture, the hexagonal Ising-like in-plane anisotropy D_{IP} stabilizes the long-range magnetic ordering, shifting $T_{N,0}$ upwards to T_N by Δ. Since the 3D character of the long-range ordering was shown by neutron scattering [5], we interpret our phase diagram as resulting from a field-induced crossover from a 3D Ising-like long-range ordering controlled by the hexagonal in-plane anisotropy D_{IP}, to a 3D Ising long-range ordering controlled by an effective field-induced in-plane anisotropy $D_{\mathrm{IP}}^{\mathrm{eff}}(\mathbf{H})$. As long as there is a distribution of domains, i.e., for $H \lesssim H^*$, $T_N(H)$ is independent of H and is not controlled by $D_{\mathrm{IP}}^{\mathrm{eff}}(\mathbf{H})$. We speculate that our phase diagram—and its interpretation—may be generic to quasi-2D systems with more than one easy axes and with $J \gg D_{XY} \gg D_{\mathrm{IP}}, J'$ [15].

In the following, we use our data, together with thermodynamic relationships, to determine the uniaxial pressure dependences of T_N, J, and H^*. The Ehrenfest relationship $\partial T_N/\partial p_i = \Delta\alpha_i V T_N/\Delta C_p$, where $\Delta\alpha_i$ and ΔC_p are the expansivity and specific heat jumps at the transition, gives the uniaxial pressure dependences of T_N. Similarly, the uniaxial pressure dependences of J can be obtained by substituting $T_{\max} \sim J$ for T_N in an Ehrenfest-type relation and considering the total magnetic signal for $\Delta\alpha$ and ΔC_p. Appropriate scalings of specific heat and thermal expansion (at $H = 0$) are shown in Figs. 4(a)–4(c) [16], and the resulting pressure dependences are listed in Table I. The hierarchy $(1/J)\partial J/\partial p \ll (1/T_N)\partial T_N/\partial p$ indicates that $\partial T_N/\partial p$ is not controlled by J. We also note the field-induced sign change of $\partial T_N/\partial p_a$ when $\mathbf{H} \parallel \mathbf{a}$. In contrast, $\partial T_N/\partial p_a$ and $\partial T_N/\partial p_c$ remain positive and negative, when $\mathbf{H} \perp (\mathbf{p}, \mathbf{c})$ and $\mathbf{H} \parallel \mathbf{a}$, respectively, over the whole investigated H range. In Fig. 4(d), the derivative of magnetization $\partial M/\partial(\mu_0 H)$, and the magnetostriction coefficient $\lambda_a^{\parallel} = (1/L_a)\partial L_a/\partial(\mu_0 H)$ measured in the longitudinal configuration, are shown at 5 K as a function of H. The data were scaled at the peak values to apply the generalized Ehrenfest relation $\partial H^*/\partial p_i = V\Delta\lambda_i/\Delta[\partial M/\partial(\mu_0 H)]$. The obtained p dependences of H^* (Table I) are much larger than the ones of T_N, which in turn are larger than those of J, and they are the largest for uniaxial pressures applied within the hexagonal plane. Since H^* depends strongly on the zero-field in-plane anisotropy, this suggests that the pressure dependence of the in-plane anisotropy controls the pressure dependence of H^*. Further, in-plane pressure effects on H^* have opposite signs parallel and perpendicular to the applied field. In the following discussion, we provide a simple explanation of the above correlations. We note that the c-axis pressure dependence of H^* is much smaller than the in-plane pressure dependences of H^* and may result from them via elastic coupling of the axes.

In the high-field phase (AF′ in Fig. 3), the spins are aligned such that their direction is perpendicular to $\mathbf{H}$. Associated with this spin-flop-like crossover is a macroscopic distortion of the hexagonal plane, which develops below T_N and can be extracted from our dilatometry data [the integration of $\alpha(T)$ and $\lambda(H)$, in Figs. 2(a), 2(b), and 4(d), leads to the length changes]. This in-plane distortion is such that the crystal contracts along the spin direction and expands perpendicularly to the spins [Fig. 2(e)]. Since presumably the magnetic domains are already distorted at low fields [17], the application of uniaxial pressure $\mathbf{p}$ in the easy plane will tend to align the spins such that the contracted direction is parallel to $\mathbf{p}$. Hence, the favored spin direction will be parallel to $\mathbf{p}$. This effect is analogous to the magnetic field effect and can be described by adding an effective pressure-induced in-plane Ising anisotropy term $D_{\mathrm{IP}}^{\mathrm{eff}}(\mathbf{p})$ to the Hamiltonian, the corresponding easy-axis being parallel to $\mathbf{p}$.

The H and T evolutions of this in-plane distortion ultimately govern the in-plane uniaxial p dependences of H^* and T_N. $\mathbf{p}$ applied along $\mathbf{a}^{\perp}$, i.e., perpendicular to ($\mathbf{H}$, $\mathbf{c}$), will favor the alignment of the spins perpendicular to $\mathbf{H}$, and thus will reduce H^*. Using $(1/H^*)\partial H^*/\partial p = -1.4$ kbar^{-1}, we estimate that 0.5 kbar along $\mathbf{a}^{\perp}$ is enough to reduce H^* to zero and to align the spins by stress alone. On the other hand, $(1/H^*)\partial H^*/\partial p$ is positive for $\mathbf{p}$ applied along $\mathbf{a}^{\parallel}$, i.e., parallel to $\mathbf{H}$, which means that larger fields will be needed to align the spins. Magnetic ordering will be favored if both the field- and the pressure-induced anisotropies $D_{\mathrm{IP}}^{\mathrm{eff}}(\mathbf{H})$ and $D_{\mathrm{IP}}^{\mathrm{eff}}(\mathbf{p})$ act cooperatively to align the

TABLE I. Normalized uniaxial pressure dependences of J, T_N, and H^* obtained from our data using Ehrenfest relations.

(kbar^{-1})		$\mathbf{p} \parallel \mathbf{a}$ $\mathbf{H} \parallel \mathbf{a}$	$\mathbf{p} \parallel \mathbf{a}$ $\mathbf{H} \perp (\mathbf{p}, \mathbf{c})$	$\mathbf{p} \parallel \mathbf{c}$ $\mathbf{H} \parallel \mathbf{a}$
$(1/J)\partial J/\partial p$	(0 T)	1.5×10^{-3}	1.5×10^{-3}	⋯
$(1/T_N)\partial T_N/\partial p$	(0 T)	1×10^{-2}	1×10^{-2}	-6×10^{-3}
	(10 T)	-5×10^{-3}	1×10^{-2}	-4×10^{-3}
$(1/H^*)\partial H^*/\partial p$		2.5	−1.4	-2.5×10^{-1}

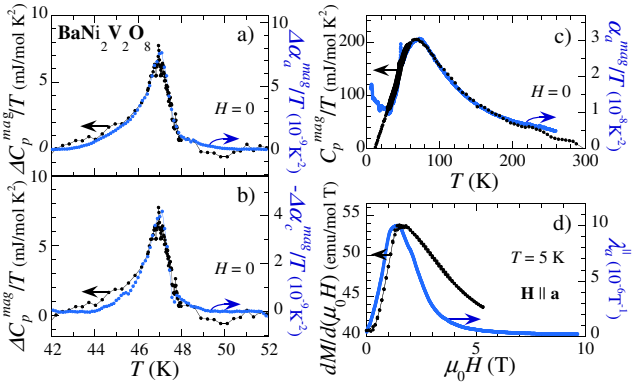

FIG. 4 (color online). (a)–(c) Scalings of specific heat and thermal expansivity (with a minus sign for the c axis) used to determine the zero-field uniaxial pressure dependences of T_N and J. (d) Scaling of $\partial M/\partial(\mu_0 H)$ and $\lambda_a^{\parallel}$ versus H at 5 K.

spins along the same axis [18]. This explains the positive value of $\partial T_N/\partial p_a^{\perp}$ at 10 T. In contrast, $D_{\mathrm{IP}}^{\mathrm{eff}}(\mathbf{p})$ acts against $D_{IP}^{\mathrm{eff}}(\mathbf{H})$ when $\mathbf{p}$ is applied along $\mathbf{a}^{\parallel}$, i.e., parallel to $\mathbf{H}$, which leads to $\partial T_N/\partial p_a^{\parallel} < 0$ at 10 T.

In conclusion, the (T, H) phase diagram of $BaNi_2V_2O_8$ was studied with $\mathbf{H} \perp \mathbf{c}$. The obtained field and uniaxial pressure dependences of T_N were interpreted as the consequence of effective field- and pressure-induced in-plane anisotropies. Our data clearly demonstrate the importance of the in-plane anisotropy for establishing 3D long-range order in $BaNi_2V_2O_8$. A search for BKT behavior should be restricted to a temperature region above T_N, where in-plane anisotropy no longer influences the growth of the 2D-XY correlations. In the limit of $D_{\mathrm{IP}} = 0$, we extrapolated a Néel temperature $T_{N,0} = 46.6$ K, which provides an upper estimate of the BKT temperature T_{BKT} [19]. Since the Ising-like anisotropy D_{IP} leads to an increase of T_N by almost 1 K, 2D-XY BKT behavior may be valid for temperatures at least several degrees higher than T_N. These results are expected to be useful for future studies of BKT behavior.

We acknowledge useful discussions with L. P. Regnault, C. Boullier, D. Reznik, T. Roscilde, J. Villain, S. Bayrakci, B. Keimer, and R. Eder. This work was supported by the Helmholtz-Gemeinschaft through the Virtual Institute of Research on Quantum Phase Transitions and Project No. VH-NG-016.

[1] *Magnetic Properties of Layered Transition Metal Compounds*, edited by L. J. DeJongh (Kluwer Academic Publishers, Dordrecht/Boston/London, 1990).
[2] V. L. Berezinskii, Zh. Eksp. Teor. Fiz. **59**, 907 (1970) [Sov. Phys. JETP **32**, 493 (1971)]; J. M. Kosterlitz and D. J. Thouless, J. Phys. C **6**, 1181 (1973).
[3] P. Minnhagen, Rev. Mod. Phys. **59**, 1001 (1987).
[4] A. Cuccoli *et al.*, Phys. Rev. B **67**, 104414 (2003).
[5] N. Rogado *et al.*, Phys. Rev. B **65**, 144443 (2002).
[6] M. Heinrich *et al.*, Phys. Rev. Lett. **91**, 137601 (2003).
[7] Two spin wave gaps $\Delta_{XY} \simeq 3$ and $\Delta_{\mathrm{IP}} \simeq 0.2$ meV, related to the XY and in-plane anisotropies, respectively, were recently measured by neutron scattering [D. Reznik, S. Bayrakci, J. Lynn, and B. Keimer (private communication)]; using $J \simeq 10$ meV and $\Delta_i \propto \sqrt{D_i J}$, we estimate $D_{XY} \simeq 1$ and $D_{\mathrm{IP}} \simeq 4 \times 10^{-3}$ meV (to our knowledge, no experiment was able to estimate J').
[8] In W. Knafo *et al.*, J. Magn. Magn. Mater. **310**, 1248 (2007), a slight increase of T_N for $\mathbf{H} \parallel \mathbf{c}$ was associated to a field-induced XY anisotropy.
[9] The procedure proposed in J. C. Lashley *et al.*, Cryogenics **43**, 369 (2003) was used to enhance resolution.
[10] The phonon contribution is assumed to be similar in both $BaNi_2V_2O_8$ and $BaNi_{0.8}Mg_{1.2}V_2O_8$, while the magnetic contribution of $BaNi_{0.8}Mg_{1.2}V_2O_8$ has a weight only at very low temperatures.
[11] We recall that in Ref. [5], a "small feature" was observed at $T_N \simeq 48$ K in the specific heat, the associated entropy being estimated by $\Delta S_N/\Delta S_{\mathrm{mag}} \simeq 8 \times 10^{-3}$.
[12] P. Bloembergen, Physica (Amsterdam) **85B**, 51 (1977).
[13] Here, the spins align $\perp \mathbf{H}$; ultimately, for $\mu_0 H \gg 10$ T, the antiferromagnetic phase will be replaced by a polarized state with the spins $||\mathbf{H}$. An introduction about effective field-induced anisotropy can be found in Ref. [1].
[14] This picture has been proposed in J. Villain and J. M. Loveluck, J. Phys. (Paris) **38**, L77 (1977) for quasi-1D magnetic systems in a magnetic field.
[15] Such phase diagrams were already obtained in I. W. Sumarlin *et al.*, Phys. Rev. B **51**, 5824 (1995) and B. J. Suh *et al.*, Phys. Rev. Lett. **75**, 2212 (1995) on the quasi-2D tetragonal magnetic systems Pr_2CuO_4 and $Sr_2CuO_2Cl_2$, respectively. While Sumarlin *et al.* did not discuss the increase of $T_N(H)$, Suh *et al.* introduced a picture with a field-induced crossover from XY- to Ising-driven Néel ordering, which is quite different from our interpretation of the phase diagram. In Y. Shapira *et al.*, Phys. Rev. B **21**, 1271 (1980), a similar phase diagram was obtained for the 3D hexagonal $CsMnF_3$, being interpreted as a XY to Ising crossover (as in Suh *et al.*). An increase of $T_N(H)$ was also reported for quasi-2D systems with a single easy axis [1], although their phase diagram is somewhat different than ours (first order spin-flop transition instead of a spin alignment crossover).
[16] The magnetic contribution to the thermal expansion of Fig. 4(a) is estimated using $\alpha_{\mathrm{mag}} = \alpha - \alpha_{\mathrm{ph}}$, where $\alpha_{\mathrm{ph}} = C_{\mathrm{ph}} \times s$ is the phononic contribution, s being a constant refined so that $\alpha_{\mathrm{mag}}(T)$ and $C_{\mathrm{mag}}(T)$ have the same shape. The peaks at T_N plotted in Figs. 4(b) and 4(c) were extracted using appropriate backgrounds.
[17] A distortion relative to the spin direction characterizes certainly each magnetic domain at $H = 0$, but is not observed macroscopically because of averaging over all domains. For $\mathbf{H} \perp \mathbf{c}$, the formation of a single domain due to spin alignment is believed to induce the macroscopic distortion observed experimentally.
[18] Here both $\mathbf{p} \parallel \mathbf{a}$ and $\mathbf{H} \perp (\mathbf{a}, \mathbf{c})$ favor an alignment of the spins parallel to $\mathbf{a}$.
[19] This is compatible with $T_{\mathrm{BKT}} = 43.3$ K estimated from a fit of the ESR linewidth in Ref. [6] (where $T_N \simeq 50$ K was also obtained, instead of 47.4 K here).